Heat capacity of hexagonal boron nitride sheet in Holstein model

© Hamze Mousavi*,+¶

* Department of Physics, Razi University,
Kermanshah, Iran
+ Nano Science and Nano Technology Research Center, Razi University,
Kermanshah, Iran

(Получена 22 ноября 2012 г. Принята к печати 26 августа 2013 г.)

The effects of electron-phonon interaction on the electronic heat capacity of hexagonal boron nitride plane are investigated within the Holstein Hamiltonian model and Green's function formalism. By using different electron-phonon coupling constants of boron and nitrogen sublattices, it is found that the specific heat has different behaviors in two temperature regions. In the low temperature region, the electron-phonon interaction causes the enhancement of specific heat due to decreasing the band gap, while heat capacity reduces in the high temperature region because of decreasing the excitation spectrum.

Boron nitride (BN) structures are fascinating low-dimensional objects that offer an outstanding playground to challenge the quantum theory at the nanoscale and manifesting novel physical phenomena. BN sheet in hexagonal form is analogous to graphene where boron (B) and nitrogen (N) atoms can be replaced by carbon atoms but its property is quite different. Theoretical studies suggest that BN sheet is a wide gap semiconductor with electronic band gap, $\varepsilon_g \approx 5.5$ eV [1,2]. Since the electronic property of BN sheet is strongly connected to the delocalised electron system, obviously any modification of these systems will influence these properties. Consequently, by the proper choice of the type of modification the electronic properties can be deliberately tuned. The tuning of the electronic properties could be referred to as electron-phonon (EP) interaction. The interaction between electrons and phonons is actually the correction of coulomb interaction between electrons and ions due to vibration of ions. Conduction electrons suffer an effective retarded interaction by propagation of phonons and provided to the phonons react instantaneously, the effective interaction is no longer retarded. Therefore, we see that the maps onto an attractive Hubbard model [3].

Knowledge of EP coupling is essential for the understanding of many properties of nanostructures that it would be dominated by contribution of phonons. For instance, the heat capacity is a quantity which directly reflects the details of the excitation spectrum. So, it is important how the electronic specific heat capacity of the system, C, is affected by the EP coupling strength. Therefore, it is necessary to understand the lattice dynamics of the system under consideration, especially in the low phonon frequency regime. Phonons and thermodynamics properties in BN structures have been an active area of research in recent years [4–6]. For example, specific heat capacity has been measured by Zhi et al. [4]. They have calculated the specific heat capacity for multi-walled BN nanotubes (BNNTs) synthesized by chemical vapor deposition and using boron and metal oxide as precursor. An *ab initio* study of electron mobility and EP coupling in chemically modified graphene as well as hexagonal boron carbon nitrogen was investigated by Bruzzone and Fiori [5].

¶ E-mail: hamze.mousavi@gmail.com

Lattice interaction model including short-range coupling have been discussed in Holstein model [7,8]. In this model, dynamics interaction is characterized by a short-range EP interaction and tight-binding electrons couples to the optical phonon modes locally. The key factors determining the EP coupling strength are the EP matrix elements between the initial and the final electronic states close to the Fermi level. In other words, it is clear that the EP interaction strength depends on the orbital characteristics of the initial and final electronic states as well as the displacement pattern of the phonon modes. Also, the optical out-of-plane modes (ZO) are energetically smaller than in-plane vibrations due to the hybridization of the sp^2-orbitals of the system. The purpose of this work is to study the EP interaction effects, i. e., ZO phonon, on the DOS as well as electronic heat capacity of BN plane using the Green's function method. Since the inertia of the ions is important, the interaction between electrons which is mediated by phonons, is not instantaneous but retarded. This makes Green's function a particularly useful tool for describing the effect of the EP interaction. So, we study the DOS and the specific heat of the system by the Green's function approach taking to account the EP interaction.

The Hamiltonian of model can be written as, $\mathscr{H} = \mathscr{H}_{\rm e} + \mathscr{H}_{\rm ph} + \mathscr{H}_{\rm e\text{-}ph}$, where $\mathscr{H}_{\rm e}$, $\mathscr{H}_{\rm ph}$ and $\mathscr{H}_{\rm e\text{-}ph}$ are the electron, phonon and e-ph interaction terms, respectively. In the second quantisation, the considered Hamiltonian is as follows [9],

$$\mathscr{H} = -\sum_{ij\alpha\beta} t_{ij}^{\alpha\beta} a_i^{\alpha\dagger} a_j^{\beta} + \sum_{i\alpha} \varepsilon_0^{\alpha} a_i^{\alpha\dagger} a_i^{\alpha} + \sum_{i\alpha} \omega_0^{\alpha} b_i^{\alpha\dagger} b_i^{\alpha} + \sum_{i\alpha} g_0^{\alpha} \left(b_i^{\alpha\dagger} + b_i^{\alpha}\right) a_i^{\alpha\dagger} a_i^{\alpha}, \quad (1)$$

where α and β refer to the B or N sites inside of the graphene Bravais lattice unit cell (Fig. 1). $t_{ij}^{\alpha\beta}$ denotes the amplitude for a π electrons to hop from site α in the unit cell i to the site β in the nearest-neighbor unit cell j; $\varepsilon_{0i}^{\alpha}$ shows the on-site energy of sub-site α in the Bravais lattice unit cell i. It takes ε_0 $(-\varepsilon_0)$ for B (N) atoms in the systems. $a_i^{\alpha\dagger}$ (a_i^{α}) displays the electron creation (annihilation) operator at the sub-site α in the Bravais

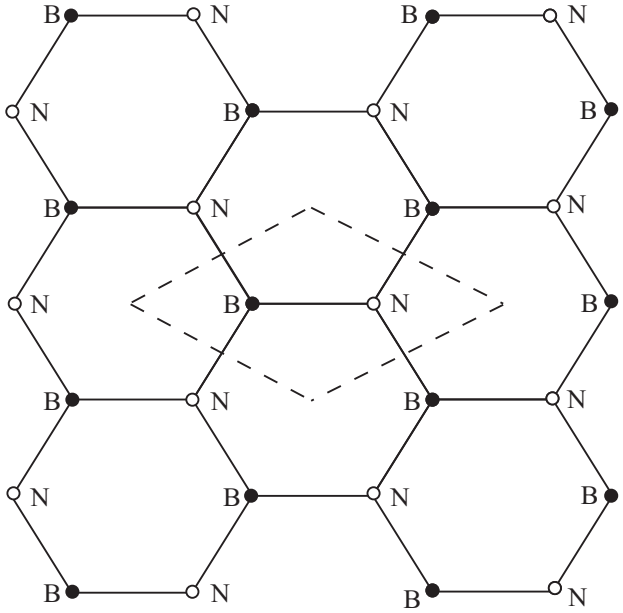

Figure 1. Schematic presentation of BN sheet. The light dashed lines illustrate the Bravais lattice unit cell. Each cell includes two nonequivalent sites, which are denoted by B and N.

lattice unit cell i and $b_i^{\alpha\dagger}$ (b_i^{α}) describes corresponding bosonic operator. ω_0^{α} exhibits dispersionless frequency of the sub-site α in the Bravais lattice unit cell i and g_0^{α} indicates on-site EP coupling strength at the sub-site α in the the Bravais lattice unit cell i. In our calculations we take the chemical potential $\mu = 0$, which corresponds to contribution of one electron per p_z orbital in the system. We assume the unit such that $\hbar = k_B = 1$ (k_B is Boltzmann constant).

Because of the existence of two atoms in the Bravais lattice unit cell, the Green's function needs to be written as a 2×2

$$\mathbf{G}(i, j; \tau) = \begin{pmatrix} G^{\mathrm{BB}}(i, j; \tau) & G^{\mathrm{BN}}(i, j; \tau) \\ G^{\mathrm{NB}}(i, j; \tau) & G^{\mathrm{NN}}(i, j; \tau) \end{pmatrix},$$

with $G^{\alpha\beta}(i, j; \tau) = -\langle \mathscr{T} a_i^{\alpha}(\tau) a_j^{\beta\dagger}(0) \rangle$ where τ hints the imaginary time and $\mathscr{T}$ remarks the time ordering operator. Here, $\langle \cdots \rangle$ plays as ensemble averaging on the ground state of the system. Using the Hamiltonian in Eq. (1), Heisenberg equation, $\partial a_i^{\alpha}(\tau)/\partial\tau = [a_i^{\alpha}(\tau), \mathscr{H}(\tau)]$ and calculating $\partial G^{\alpha\beta}(i, j; \tau)/\partial\tau$, the equation of motion for the electron and phonon operators can be obtained as,

$$a_i^{\alpha\dagger} a_i^{\alpha} = \frac{1}{g_0^{\alpha}} \frac{\partial b_i^{\alpha}}{\partial \tau} - \frac{\omega_0^{\alpha}}{g_0^{\alpha}} b_i^{\alpha}, \tag{3}$$

so, the equation of motion gets the shape,

$$\sum_l \left\{ -\delta_{il} \left[\mathbf{I} \frac{\partial}{\partial \tau} + \boldsymbol{\varepsilon}_{0i} + \boldsymbol{\Gamma}_i(\tau) \right] + \mathbf{t}_{il} \right\} \mathbf{G}(l, j; \tau) = \delta(\tau) \delta_{ij} \mathbf{I}, \tag{4}$$

where δ_{il} (δ_{ij}) presents the Kronecker symbol, $\mathbf{I}$ serves as a 2×2 unit matrix, a Dirac δ-function is introduced by $\delta(\tau)$.

Also, $\boldsymbol{\varepsilon}_{0i}$, $\boldsymbol{\Gamma}_i(\tau)$ and $\mathbf{t}_{il}$ matrixes are defined by,

$$\boldsymbol{\varepsilon}_{0i} = \begin{pmatrix} \varepsilon_{0i}^{B} & 0 \\ 0 & \varepsilon_{0i}^{N} \end{pmatrix}, \tag{5}$$

$$\boldsymbol{\Gamma}_i(\tau) = \begin{pmatrix} \eta^B \langle a_i^{B\dagger}(\tau) a_i^B(\tau) \rangle & 0 \\ 0 & \eta^N \langle a_i^{N\dagger}(\tau) a_i^N(\tau) \rangle \end{pmatrix}, \tag{6}$$

and

$$\mathbf{t}_{il} = \begin{pmatrix} t_{il}^{BB} & t_{il}^{BN} \\ t_{il}^{NB} & t_{il}^{NN} \end{pmatrix} \tag{7}$$

respectively. In the Eq. (6), $\eta^{\alpha} \equiv 2(g_0^{\alpha})^2/\omega_0^{\alpha}$. Using an imaginary time Fourier transformation,

$$\mathbf{f}(\tau) = \frac{1}{\boldsymbol{\beta}} \sum_m e^{-\imath\omega_m \tau} \mathbf{f}(\imath\omega_m), \tag{8}$$

and following relation,

$$\frac{1}{\boldsymbol{\beta}} \int_0^{\boldsymbol{\beta}} d\tau\, e^{\imath(\omega_m - \omega_{m'})\tau} = \delta_{mm'}, \tag{9}$$

we obtain that,

$$\sum_l \left\{ [\imath\omega_m \mathbf{I} + \boldsymbol{\varepsilon}_{0i} + \boldsymbol{\Gamma}_i(\imath\omega_m)]\, \delta_{il} + \mathbf{t}_{il} \right\} \mathbf{G}(l, j; \imath\omega_m) = \delta_{ij} \mathbf{I}, \tag{10}$$

in which $\boldsymbol{\beta} = T^{-1}$ performs as the inverse of temperature, $\omega_m = \pi(2m + 1)T$ are the fermionic Matsubara frequencies and $\{m, m'\}$ denote integer numbers. Analytical continuation, $\imath\omega_m \to E = \mathscr{E} + \imath 0^+$, of Eq. (10) leads to the following equation,

$$\sum_l \left[E\mathbf{I} + \boldsymbol{\varepsilon}_{0i} + f(\mathscr{E}, T)\boldsymbol{\eta} + \mathbf{t}_{il} \right] \mathbf{G}(l, j; E) = \mathbf{I}\delta_{ij}, \tag{11}$$

so that $f(\mathscr{E}, T) = [1 + \exp(\mathscr{E}/T)]^{-1}$ notifies the Fermi-Dirac distribution function and $\boldsymbol{\eta}$ matrix is defined as,

$$\boldsymbol{\eta} = \begin{pmatrix} \eta^B & 0 \\ 0 & \eta^N \end{pmatrix} \tag{12}$$

The $\mathbf{k}$-space Fourier transformation of Eq. (11) leads to the following relation,

$$\mathbf{G}(i, j; E) = \frac{1}{\mathscr{N}} \sum_{\mathbf{k}} e^{\imath \mathbf{k} \cdot \mathbf{r}_{ij}} \left[E\mathbf{I} + \boldsymbol{\varepsilon}_0 + f(\mathscr{E}, T)\boldsymbol{\eta} - \boldsymbol{\epsilon}_{\mathbf{k}} \right]^{-1}, \tag{13}$$

in which $\mathscr{N}$ presents number of the Bravais lattice unit cell, $\mathbf{k} = (k_x, k_y)$ refers to two-dimensional wave vector in the first Brillouin zone, $\mathbf{r}_{ij}$ are three vectors that connect a B (N) site to it's nearest neighbors N (B) sites and $\boldsymbol{\epsilon}_{\mathbf{k}}$ plays the Fourier transformation of $\mathbf{t}_{ij}$,

$$\boldsymbol{\epsilon}_{\mathbf{k}} = t \times \begin{pmatrix} 0 & e^{\imath k_x a_0} + 2e^{-\imath k_x \frac{a_0}{2}} \cos(\sqrt{3} k_y \frac{a_0}{2}) \\ e^{-\imath k_x a_0} + 2e^{\imath k_x \frac{a_0}{2}} \cos(\sqrt{3} k_y \frac{a_0}{2}) & 0 \end{pmatrix}, \tag{14}$$

where $t \equiv t_{\langle ij \rangle}^{BN} = t_{\langle ij \rangle}^{NB}$, $\langle ij \rangle$ implies the nearest neighbor sites in the Bravais lattice unit cell i and j and a_0 expresses interatomic distance. The DOS of system can written by

following relation,

$$D(\mathscr{E}) = -\frac{1}{2\pi}\,\Im\left[G^{BB}(i,i;E) + G^{NN}(i,i;E)\right], \qquad (15)$$

where $G^{\alpha\alpha}(i,i;E)$ can be obtained from Eq. (13). Also, the electronic specific heat capacity reads as [10],

$$C = \int_{-\infty}^{+\infty} d\mathscr{E} D(\mathscr{E}) \mathscr{E} \frac{\partial f(\mathscr{E},T)}{\partial T}. \qquad (16)$$

In summary, we want to consider how the DOS and electronic heat capacity of hexagonal BN sheet affected by EP. We used the Green's function technique, Holstein model and standard mean field theory. We set coupling strength of B and N sublattices as $\eta^{\mathrm{B}} = 0.50\eta^{\mathrm{N}}$, $\eta^{\mathrm{B}} = 1.0\eta^{\mathrm{N}}$ and $\eta^{\mathrm{B}} = 2.0\eta^{\mathrm{N}}$ in which $\eta^{\mathrm{N}} = 0.15t$ and hopping integral to the first nearest neighbors is $t = 2.9\,\mathrm{eV}$ [11–13]. We also set the on-site energy of B and N atoms as, $\varepsilon_0 = +0.80t$ and $-0.80t$ [11–15]. We note that coupling constant is small due to the low DOS in the system. Figs. 2 and 3 illustrate the results. In Fig. 2, the DOS of the system is plotted in the cases of without EP interaction and with EP. We see that the band gap of BN plane decreases with increasing EP interaction. It is independent from individual values of η^{B} or η^{N} but depends on total value of coupling strength. In semiconductors, the EP coupling causes the increasing quasiparticle weight and band gap decreases. This is in contrast to metals where an increase of the EP coupling, decreases quasiparticle weight of electron excitation [3,13]. We also investigate the effect of EP on the heat capacity of BN sheet using Eqs. (8) and (9). In Fig. 3, electronic heat capacity of the system is plotted for mentioned values of η. As we noted, the heat capacity is a quantity which directly depends on the details of the excitation spectrum and the band gap of aystem decreases because of EP interaction. Furthermore, it is well-known that the heat capacity of semiconductors, in the low temperature, can be written as [16], $C \propto \exp(-\mathscr{E}_g/T)$. According to this formula, with decreasing $\mathscr{E}_g$, the specific heat increases in the low temperature region as it is shown in Fig. 3. On the other hand, the specific heat decreases with increasing η in the high temperature region. In this region, for temperature increasing of the system, less value of energy is needed rather than low temperature region. Therefore from general formula of the specific heat, $C = \partial U/\partial T$, the electronic specific heat capacity of the system reduces with increasing η.

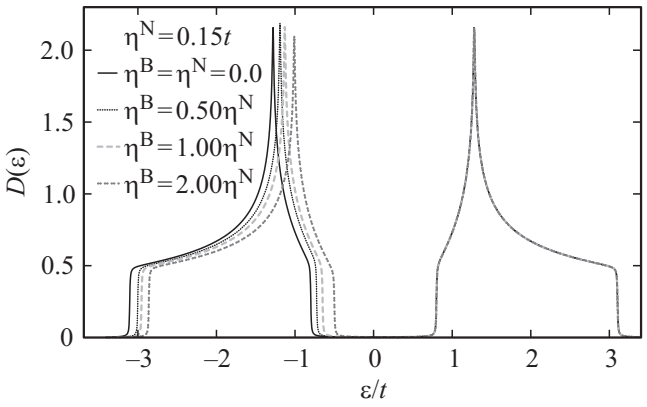

Figure 2. DOS of BN plane without EP interaction (solid line) and with EP coupling (dashed lines). The band gap decreases with increase of coupling strength.

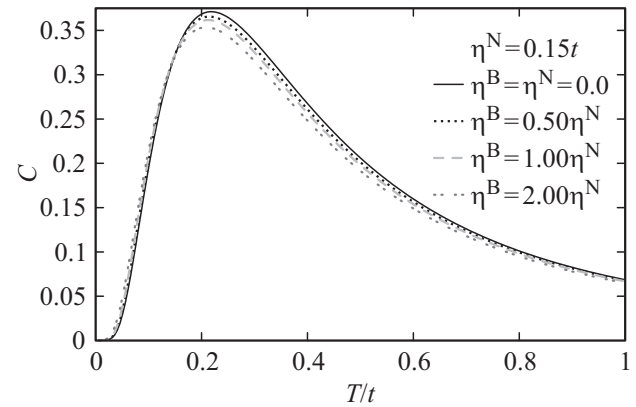

Figure 3. The specific heat of BN sheet in terms of temperature without EP (solid line) and with EP interaction (dashed lines). The specific heat changes with the strength of EP coupling in two temperature regions.

So it is concluded that with increasing EP coupling strength, the band gap of the system decreases due to increasing quasiparticle weight and the specific heat has different behaviors in two temperature regions. In the low temperature region, the EP interaction causes the enhancement of specific heat due to decreasing the band gap, while heat capacity decreases in the high temperature region due to decreasing the excitation spectrum.

References

[1] X. Blasé, A. Rubio, S.G. Louie, M.L. Cohen. Euro. Phys. Lett., **28**, 335 (1994).
[2] A. Rubio, J.L. Corkill, M.L. Cohen. Phys. Rev. B, **49**, 5081 (1994).
[3] A. Georges, G. Kotliar, W. Krauth, M.J. Rozenberg. Rev. Mod. Phys., **68**, 13 (1996).
[4] C. Zhi, Y. Bando, C. Tang, D. Golberg. Solid State Commun., **151**, 183 (2011).
[5] S. Bruzzonea, G. Fiori. Appl. Phys. Lett., **99**, 222108 (2011).
[6] T. Tohei, A. Kuwabara, F. Oba, I. Tanaka. Phys. Rev. B, **73**, 64304 (2006).
[7] T. Holstein. Ann. Phys., **8**, 3252 (1959).
[8] T. Holstein. Ann. Phys., **8**, 343 (1959).
[9] H. Mousavi. Commun. Theor. Phys., **57**, 482 (2012).
[10] N.W. Ashcroft, N.D. Mermin. *Solid State Physics* (Harcourt Brace College Publishers, 1976).
[11] R.Q. Wu, L. Liu, G.W. Peng, Y.P. Feng. Appl. Phys. Lett., **86**, 122 510 (2005).
[12] R.B. Chen, F.L. Shyu, C.P. Chang, M.F. Lin. J. Phys. Soc. Jpn., **71**, 2286 (2002).
[13] R.B. Chen, C.P. Chang, F.L. Shyu, M.F. Lin. Solid State Commn., **123**, 365 (2002).
[14] T. Yoshioka, H. Suzuura, T. Ando. J. Phys. Soc. Jpn., **72**, 2656 (2003).
[15] M. Capone, S. Ciuchi. Phys. Rev. Lett., **91**, 186 405 (2003).
[16] C. Kittel. *Introduction to Solid State Physics* (Wiley, New York, 2004).

Редактор Т.А. Полянская